J|A|C|S
ARTICLES

Published on Web 10/20/2010

The Origin of Charge Localization Observed in Organic Photovoltaic Materials

James E. Johns, Eric A. Muller, Jean M. J. Frechet, and Charles B. Harris*

Department of Chemistry, University of California Berkeley,
Berkeley, California 94720, United States

Received July 27, 2010; E-mail: cbharris@berkeley.edu

Abstract: Two of the primary hurdles facing organic electronics and photovoltaics are their low charge mobility and the inability to disentangle morphological and molecular effects on charge transport. Specific chemical groups such as alkyl side chains are often added to enable spin-casting and to improve overall power efficiency and morphologies, but their exact influence on mobility is poorly understood. Here, we use two-photon photoemission spectroscopy to study the charge transport properties of two organic semiconductors, one with and one without alkyl substituents (sexithiophene and dihexyl-sexithiophene). We show that the hydrocarbon side chains are responsible for charge localization within 230 fs. This implies that other chemical groups should be used instead of alkyl ligands to achieve the highest performance in organic photovoltaics and electronics.

Introduction

Charge and exciton dynamics play a dominant role in the performance and efficiency of photovoltaics, field effect transistors, and light emitting diodes. Molecular organic and polymeric materials have the potential for the production of low cost and easily processed devices. A serious limitation, however, is their susceptibility to charge localization and reduced mobility as compared to their inorganic counterparts. Conduction through hopping of localized states such as small polarons can result in a mobility decrease of up to 10^4 relative to band transport, and the energy lost to the charge stabilization reduces the open circuit voltage and efficiency of organic photovoltaics. If charge localization could be avoided or reduced in these systems, then device performance would be significantly enhanced.

One of the most studied systems with efficient transport is the alkyl-substituted polythiophene/fullerene (poly-3-hexylthiophene/phenyl-C61-butyric acid methyl ester or P3HT/PCBM) system developed by Heeger and co-workers.[1−5] It is important to note that substitution of the polythiophene by linear hydrocarbons (usually *n*-hexane) is necessary to increase solubility in organic solvents for spin-casting devices. Hydrocarbon substitution also improves solid-state miscibility with fullerenes for use in the P3HT/PCBM class of organic solar cells. Additionally, hydrocarbon substitution of the thiophene rings is thought to account for structural and morphological changes that enhance charge transport.[3,6] The observed improvement in long-range order is attributable to competitive van der Waal's interactions between the *n*-hexyl or hydrocarbon ligands and the sexithiophene aromatic moieties. This tends toward aggregating similar functional groups and decreasing disorder, while still leaving π-stacked thiophene channels for higher charge mobility.

Despite these enhancing characteristics, the mobility of P3HT is only 3×10^{-4} and 1.5×10^{-4} $\mathrm{V/cm^2 \cdot s}$ for holes and electrons, respectively, a value consistent with diffusive polaron migration.[7] Moreover, these solubilizing side chains are necessary for solution processing and spin-casting for most of the highly conjugated organic chromophores currently being investigated to replace polythiophene.[8−10] What is interesting and important about the mixed hydrocarbon/aromatic systems is whether or not the hydrocarbon part of the molecule plays a direct role in charge localization and whether the aromatic moiety alone or with a different substitution could be structured to show significantly larger mobilities. Neat aliphatic hydrocarbons have been to shown to be ubiquitous in forming small polarons.[11] It is plausible, however, that even in systems in which alkyl substitutions improve charge mobility, alkyl substitution may also impose an additional upper bound on device performance by creating localized, persistent, self-trapped charges with low mobilities.

Unfortunately, charge localization in these materials can be difficult to study because it occurs on the subpicosecond time scale. Typically, these systems are studied using ultrafast

---

(1) Kim, J. Y.; Lee, K.; Coates, N. E.; Moses, D.; Nguyen, T. Q.; Dante, M.; Heeger, A. J. *Science* **2007**, *317*, 222–225.

(2) Hwang, I. W.; Soci, C.; Moses, D.; Zhu, Z. G.; Waller, D.; Gaudiana, R.; Brabec, C. J.; Heeger, A. J. *Adv. Mater.* **2007**, *19*, 2307–2312.

(3) Kline, R. J.; McGehee, M. D. *Polym. Rev.* **2006**, *46*, 27–45.

(4) Waldauf, C.; Scharber, M. C.; Schilinsky, P.; Hauch, J. A.; Brabec, C. J. *J. Appl. Phys.* **2006**, *99*, 104503104503−6.

(5) Yang, F.; Shtein, M.; Forrest, S. R. *Nat. Mater.* **2005**, *4*, 37–41.

(6) Kline, R. J.; McGehee, M. D.; Kadnikova, E. N.; Liu, J.; Frechet, J. M. J.; Toney, M. F. *Macromolecules* **2005**, *38*, 3312–3319.

(7) Choulis, S. A.; Kim, Y.; Nelson, J.; Bradley, D. D. C.; Giles, M.; Shkunov, M.; McCulloch, I. *Appl. Phys. Lett.* **2004**, *85*, 3890–3892.

(8) Günes, S.; Neugebauer, H.; Sariciftci, N. S. *Chem. Rev.* **2007**, *107*, 1324–1338.

(9) Bundgaard, E.; Krebs, F. C. *Sol. Energy Mater. Sol. Cells* **2007**, *91*, 954–985.

(10) Zhan, X. W.; Tan, Z. A.; Domercq, B.; An, Z. S.; Zhang, X.; Barlow, S.; Li, Y. F.; Zhu, D. B.; Kippelen, B.; Marder, S. R. *J. Am. Chem. Soc.* **2007**, *129*, 7246–7247.

(11) Ge, N. H.; Wong, C. M.; Lingle, R. L.; McNeill, J. D.; Gaffney, K. J.; Harris, C. B. *Science* **1998**, *279*, 202–205.

10.1021/ja1066866

transient absorption, and absorption due to localized charge complexes (excitons, polarons, or polaron pairs) occurs over a broad spectrum in the visible to near-infrared (650−1300 nm).[12] The dynamics in different spectral regions can then be correlated with anisotropy and photoluminescence decay to infer which species corresponds to a specific wavelength. These experiments, however, do not provide any information about the nature of these states and typically suffer from many overlapping bands. They do not actually measure or determine the spatial degree of localization or the energy lost during this process.

A particularly powerful technique designed for studying the dynamics and localization of electrons at interfaces and in thin films is angular and time-resolved two photon photoemission (TPPE).[13] In this technique, a femtosecond pulse is used to excite an electron from below the Fermi level of a metal into an unoccupied molecular orbital or image potential state (IPS) of a thin film organic layer adsorbed on the metal. A second femtosecond pulse photoemits it from the layer, and the angle, delay time, and energy are measured and used to probe the material's response to the injected electron. The technique can be used to determine the time-dependent band dispersion and binding energy. The electron's effective mass is determined from the band curvature and is a measure of electron localization. Herein, TPPE is used to photoinject an electron into a delocalized excited state in an ultrathin film of two organic semiconductors, one with aliphatic side chains and one without. The effective mass is calculated from the angle resolved band structure at different times and used as a direct probe for charge localization. The results from this measurement are then used to extract the dynamic role that these ubiquitous side chains have on charge mobility and open circuit voltages in organic photovoltaics.

Experimental Section

Tunable broadband femtosecond optical pulses were produced in a commercial oscillator, regenerative amplifier, and optical parametric amplifier (Coherent Verdi-18, Mira 900F, Rega9000, and OPA9400). The pulses were then frequency doubled in a 0.1 mm type II BBO crystal and split from the fundamental with a dichroic mirror. The beams were recombined at the surface of the sample in a collinear fashion. Powers at the sample were ∼3 μW for the visible pulse and ∼200 nW for the UV pulse, and the repetition rate was 225 kHz. The kinetic energy and momentum of the photoelectrons were measured in a home-built time-of-flight detector described elsewhere.[14] To acquire the band structure parallel to the surface, the angle of the sample was changed relative to the detector, which used slits to limit the angular acceptance to approximately ±1°. The parallel momentum was then determined by eq 1 where θ is the angle between the detector and the surface normal of the sample.

$$k_{\|} = \sqrt{2m_e E_{\text{kinetic}}}\sin(\theta) \tag{1}$$

α-Sexithiophene (6T) and (α,ω)-dihexyl-sexithiophene (DH6T) were purchased from Sigma Aldrich. These were loaded into a ceramic crucible inside of a Knudsen cell and degassed at 25 K below their dosing temperature for greater than 24 h to remove small gas impurities. The samples were further degassed before dosage into the main chamber at 20 K above their dosing temperature to ensure that no impurities from the heating filaments were entering the main chamber. The main vacuum chamber was kept at a pressure below 3×10^{-10} Torr, and the effusion cell was kept below 5×10^{-7} Torr. The thiophene-based molecules were deposited onto a 0.5” diameter Ag(111) single-crystal substrate of 99.99% purity purchased from MaTecK GmbH. The crystal was cleaned via cycles of 0.5 keV Ar^+ ion sputtering at 550 K followed by annealing at 725 K between each experiment. Cleanliness of the sample was checked between experiments primarily through TPPE by examining the line widths and dynamics of the $n = 1$ IPS state, the $n = 0$ surface state (S.S.), and work function. Cleanliness of the surface was also periodically checked by low energy electron diffraction (LEED) to verify a sharp hexagonal pattern for the Ag(111) surface. Angle resolved measurements were taken along the $\Gamma_{\text{bar}} \rightarrow M_{\text{bar}}$ direction, rotated by 2.5° as determined from LEED.

It was discovered during the experiment that these materials showed a rapid rate of degradation when exposed to ultrafast pulses. This degradation shifted the energy of all peaks in the spectrum to higher energy, increased the spectral width, and decreased the intensity of the signal. To avoid this, the rate of degradation was measured by taking consecutive TPPE spectra with 20 s acquisition times over the course of 30 min to 2 h. No detectable damage was done to the layer within 2 min, and so beam exposure time was limited to 30 s per scan (single time point and single angular point) while acquiring the dynamic band structure before the sample was translated.

Results and Discussion

TPPE has been used on ultrathin films of both α-sexithiophene (6T) and its alkylated analogue (α,ω)-dihexyl-sexithiophene (DH6T) as shown in Figure 1 to determine whether the alkyl chains play a role in localizing electrons in these organic semiconductors. Their adsorption geometry on Ag(111) has been determined by Duhm et al.[15,16] As illustrated in Figure 1C and D, the sexithiophene molecules pack with the aromatic axis lying parallel to the metal surface. The alkane-substituted analogue, DH6T, forms an initial wetting bilayer of molecules having the thiophene core parallel to the surface (herein called flat DH6T). Additional layers pack vertically with the aromatic rings perpendicular to the surface and the alkyl chains forming an angle of 28° to the surface (standing DH6T).

Monolayer determination was made using 2PPE to monitor the evolution work function, the peak widths, center energies of the IPS, and the disappearance of the $n = 0$ surface state for both 6T and DH6T. LEED was also used to confirm the existence of ordered structures, although the DH6T degraded rapidly under the electron beam. The temperature of the Knudsen cell was adjusted such that flux of the molecular beam resulted in a growth rate was 0.25 ML/min for DH6T. Each of the first two monolayers of DH6T resulted in clear work function shifts observable by changes of the binding energy for the $n = 1$ and $n = 2$ IPS. Following 8 min of deposition, a new gradual transition occurred in which the $n = 2$ state disappeared and the binding energy of the $n = 1$ steadily increased. The $n = 1$ IPS peak energy stopped shifting after a further 25 min of deposition. This change in deposition rate at constant flux is similar to the change in surface area/molecule expected for the flat to standing transition. Further deposition caused a decrease in the total 2PPE signal, but did not shift the energy of the peak center or change the work function.

---

(12) Guo, J.; Ohkita, H.; Benten, H.; Ito, S. *J. Am. Chem. Soc.* **2009**, *131*, 16869–16880.

(13) Harris, C. B.; Lingle, N.-H. G., R. L., Jr.; McNeill, J. D.; Wong., C. M. *Annu. Rev. Phys. Chem.* **1997**, *48*, 711–744.

(14) Padowitz, D. F.; Merry, W. R.; Jordan, R. E.; Harris, C. B. *Phys. Rev. Lett.* **1992**, *69*, 3583–3586.

(15) Duhm, S.; Salzmann, I.; Koch, N.; Fukagawa, H.; Kataoka, T.; Hosoumi, S.; Nebashi, K.; Kera, S.; Ueno, N. *J. Appl. Phys.* **2008**, *104*, 033717–033717-7.

(16) Duhm, S.; Heimel, G.; Salzmann, I.; Glowatzki, H.; Johnson, R. L.; Vollmer, A.; Rabe, J. P.; Koch, N. *Nat. Mater.* **2008**, *7*, 326–332.

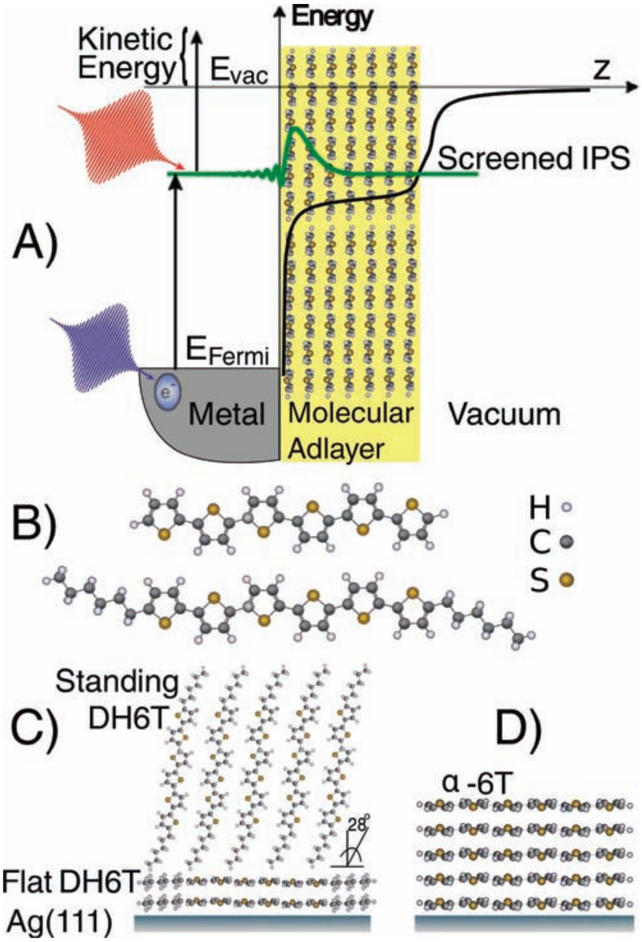

Figure 1. (A) Diagram of the TPPE experiment as performed. A UV pulse transfers an electron from below the Fermi level of Ag(111) into an initially delocalized IPS in the molecular film. After some time, Δt, a visible pulse photoemits the excited electron. Changes in the energy of the photoelectron are a result of the electron interacting with the adsorbed film. (B) Molecular structure of α-sexithiophene (top) and (α,ω)-dihexyl sexithiophene (bottom). Molecular geometries of DH6T (C) and 6T (D) adsorbed to Ag(111).

The TPPE spectra for these films are shown in Figure 2A, and the energetic referencing of the states is shown in Figure 2B. The dependence of IPS peak energy on the wavelength of light used, shown in Figure 3, was used to support the energetic assignments. The linear dependence with a slope of 1 implies that these states are energetically high above the Fermi level and can only be populated by the UV pulse.

The electronic states visible in the TPPE spectra are assigned as the screened image potential states (IPS). Image potential states are a hydrogenic series of electronic states derived from the high polarizability of metallic systems. These states are bound in the surface normal direction. The average distance from the metal surface for the first IPS is only a few angstroms, making it very sensitive to changes in its local electronic environment due to adsorbates. Parallel to the surface, these states are delocalized and behave like nearly free electrons. To monitor charge localization by side chains, it is necessary to excite charges into an initially delocalized state and watch the charge evolve. The IPS studied here is used as a delocalized, free-electron like probe, unlike the molecular states of 6T, which have been shown to be a mixture of dispersive (delocalized) and nondispersive (localized) states.[17,18] The delocalized nature of the IPS parallel to the surface makes it an excellent probe of the charge trapping power of an adsorbed film.

Localization was examined in each of the thiophene systems by monitoring the band structure and effective mass of the IPS electron. IPS electrons on ordered surfaces are highly dispersive and display an effective mass near that of a free electron. Trapping due to increased interaction with the local atoms increases the effective mass; effective masses greater than 5−10 m_e can be considered localized. In both the 6T and the DH6T films, the IPS electron is initially delocalized and has a low effective mass less than 1.6 m_e (Figure 4). For all of the morphologies except standing DH6T, the effective mass stays between 1.2 and 1.5 m_e. For coverages of DH6T beyond the wetting bilayer, the effective mass starts at 1.3 m_e, and increases to 21 ± 0.5 m_e by 233 fs. This is a signature for initially delocalized charges, which collapse or self-trap to spatially localized charges and can only move laterally by thermal activated hopping.

The amplitude of the 2PPE spectrum was also measured as a function of the parallel momentum (Figure 5). Fourier transforming the measured spectral intensity versus $k_{||}$ results in a measurement of the electronic population versus position in real space. Using the rule of thumb presented by Bezel et al. in eq 2, the spatial extent of the electron's wave function can be estimated.[19]

$$\Delta x_{\text{fwhm}} = \frac{4\ln(2)}{\Delta p_{\text{fwhm}}/\hbar} \tag{2}$$

Using this analysis, the size of the final state is estimated to be 14 ± 4 Å fwhm, which is roughly the same size as the intermolecular spacing between two adjacent DH6T molecules (6.8 Å in one direction and 7.8 Å in the other). This indicates that the electron is highly localized within the time scale of the experiment.

Lateral localization of the IPS electron can be caused by three factors. The electron can localize if the IPS couples strongly to nondispersive molecular electronic states. The electron can collapse at local defects, which perturb the periodic potential. Finally, the electron can dynamically induce an attractive polarization in the film. The resulting dynamic self-localization is the underlying mechanism for polaron formation.[11] Understanding how and why the electrons localize in organic semiconductors can lend insight into how their mobility can be improved and device performance enhanced. If the electrons are localizing purely electronically, then the aromatic portion of the molecule that contains the frontier orbitals is likely the culprit. Defect-induced localization could potentially be reduced by improved sample preparation or purification. If the localization can be identified with small polaron formation caused by coupling of the electrons to specific vibrations, then removal of the specific functional groups could remove the polaron.

Determining the mechanism for electron localization in the standing DH6T films is difficult because of the short lifetimes involved (Figure 6). With the limited angular and temporal

---

(17) Berkebile, S.; Koller, G.; Puschnig, P.; Ambrosch-Draxl, C.; Netzer, F.; Ramsey, M. *Appl. Phys. A: Mater. Sci. Process.* **2009**, *95*, 101–105.

(18) Puschnig, P.; Berkebile, S.; Fleming, A. J.; Koller, G.; Emtsev, K.; Seyller, T.; Riley, J. D.; Ambrosch-Draxl, C.; Netzer, F. P.; Ramsey, M. G. *Science* **2009**, *326*, 702–706.

(19) Bezel, I.; Gaffney, K. J.; Garrett-Roe, S.; Liu, S. H.; Miller, A. D.; Szymanski, P.; Harris, C. B. *J. Chem. Phys.* **2004**, *120*, 845–856.

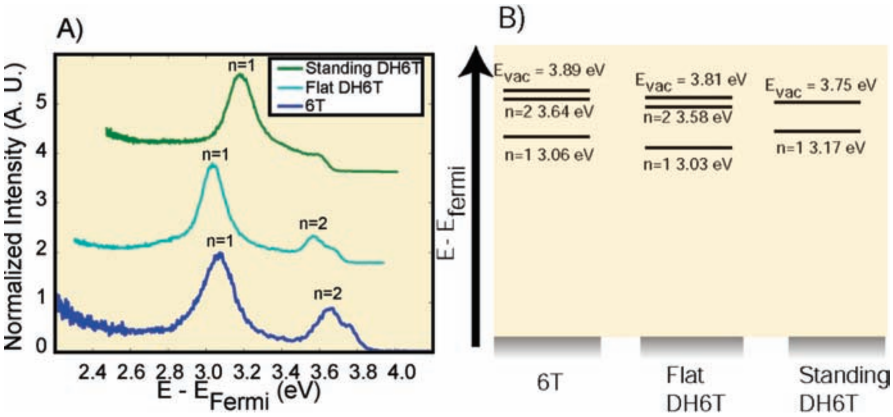

Figure 2. (A) TPPE spectra of 6T, Fflat DH6T, and standing DH6T showing the IPS. (B) Energetic positioning of the interfacial states for each film as determined experimentally.

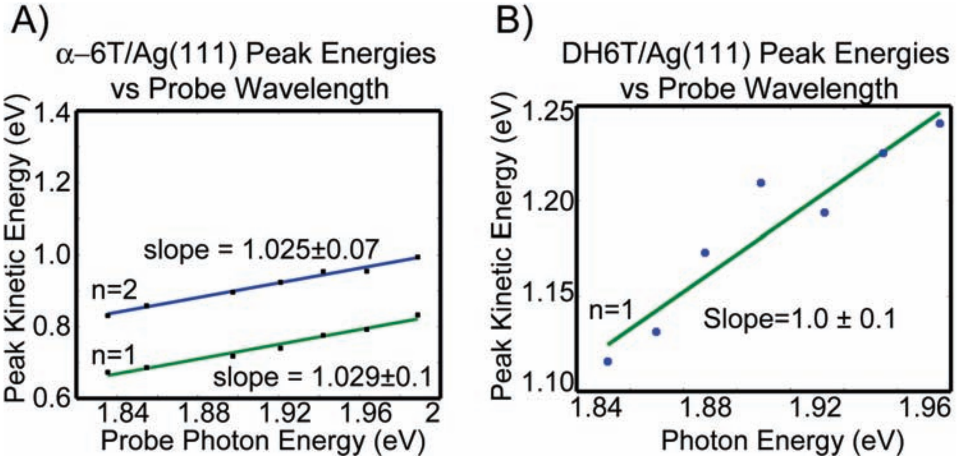

Figure 3. (A) Kinetic energy of the $n = 1$ (green) and $n = 2$ (yellow) IPS of α-sexithiophene on Ag(111). (B) Kinetic energy of the $n = 1$ for DH6T/Ag(111). A slope of 1 means that the peak is being probed by the visible pulse and the state is energetically closer to the vacuum level than the Fermi level.

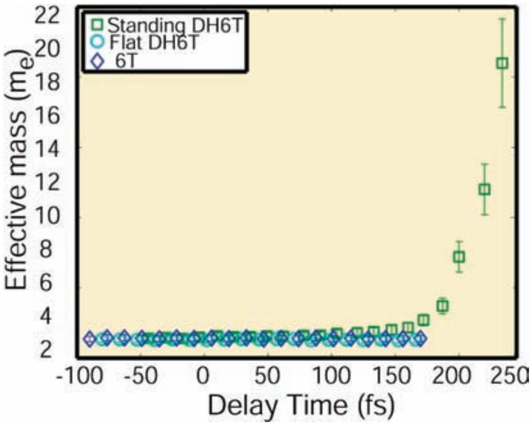

Figure 4. The effective mass of the initially delocalized IPS for each film over time. The increasing mass of the electron is direct evidence of a mobile charge localizing in the DH6T film. As the effective mass rises, the charge mobility decreases.

resolution available, only a purely electronic coupling mechanism can be strictly ruled out. The electronic mechanism requires an increase in the electronic coupling to a specific nondispersive state. Changing the orientation of the conjugated axis relative to the surface could increase the direct overlap between the IPS wave function and unoccupied electronic states of the molecule in the standing versus flat phases.[20,21] Statically localized electronic states at the interface between metals and organic semiconductors have been seen in ultrathin films of pentacene[22,23] due to strong electronic coupling. Electronic interaction with unoccupied states of the standing portion of the DH6T layer would require the electron to be on the far side of the standing hexyl groups from the metal surface (region 1 of figure 6B). Alkyl molecules have a negative electron affinity and thus present significant barriers to IPS electrons attempting to decay back into the metal. This barrier has been shown to increase the lifetime of an IPS electron to the 1−100 ps regime.[13] Instead, the measured lifetime of the localizing IPS electron is only 80 ± 30 fs. The small observed lifetime indicates that the electron is still close to the metal surface and rules out localization due to the electronic coupling mechanism.

Distinguishing between an electron trapped into a defect site and a self-localizing small polaron is also made difficult because of the short lifetime. Localization by defects has been shown to occur on the hundred femtosecond time scale in some

---

(20) Berthold, W.; Hofer, U.; Feulner, P.; Menzel, D. *Chem. Phys.* **2000**, *251*, 123–132.
(21) Gaffney, K. J.; Wong, C. M.; Liu, S. H.; Miller, A. D.; McNeill, J. D.; Harris, C. B. *Chem. Phys.* **2000**, *251*, 99–110.
(22) Yang, Q. X.; Muntwiler, M.; Zhu, X. Y. *Phys. Rev. B* **2009**, *80*, 115241–115249.
(23) Muntwiler, M.; Yang, Q.; Tisdale, W. A.; Zhu, X. Y. *Phys. Rev. Lett.* **2008**, *101*, 196403–16407.

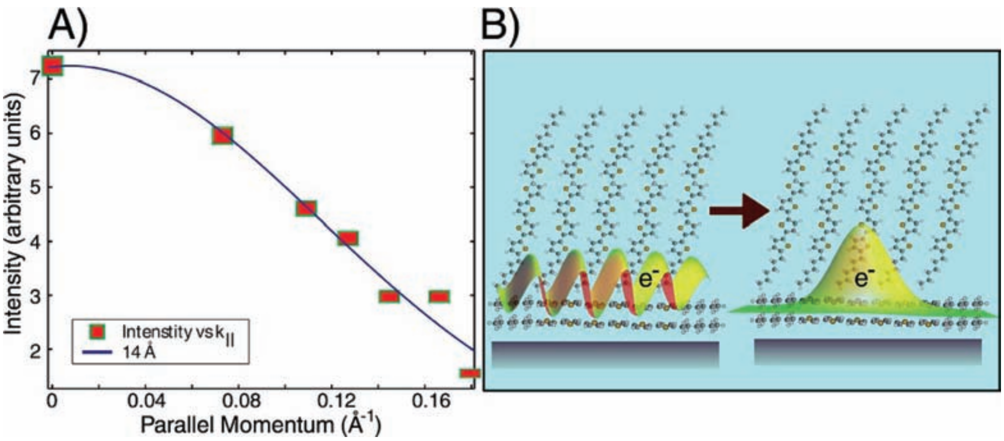

Figure 5. (A) Momentum distribution of the final localized IPS in standing DH6T. Error bars are approximately the size of the boxes as drawn. Fourier transforming the momentum distribution shows that the electron is localized to 14 ± 4 Å. (B) The localization process is schematically illustrated in the right panel.

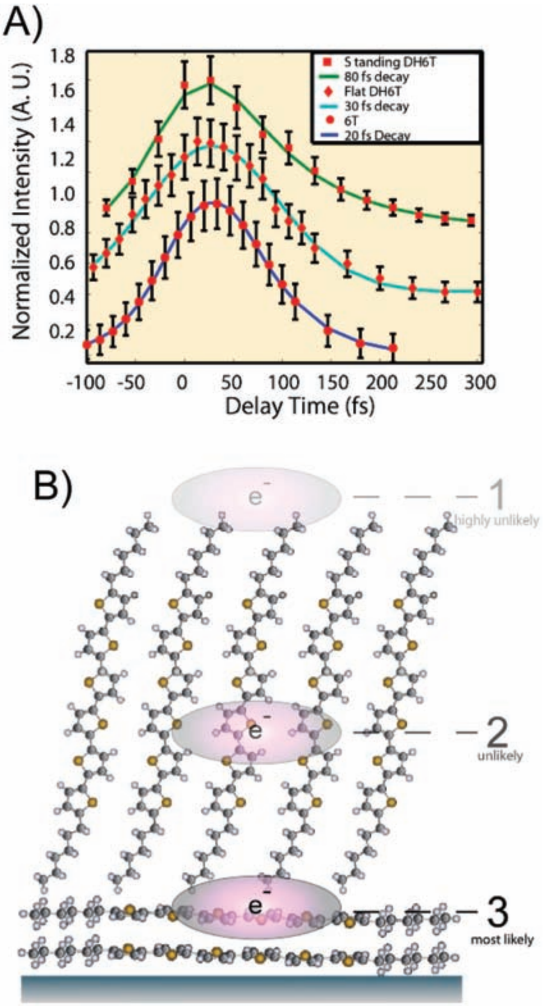

Figure 6. (A) Dynamics of the IPS electron for 6T, flat DH6T, and standing DH6T. The two-pulse cross correlation was kept below 100 fs as measured by fitting the decay of the clean Ag(111) surface state, which is a virtual transition. This state was also used to fix $t = 0$ to ±10 fs. (B) Schematic depiction of three possible average distances of the localized electron from the metal surface for DH6T. Each alkyl unit imposes a barrier to the electron tunneling back into the metal, and thus substantially increases the lifetime of the IPS electron. Because of the subpicosecond decay times shown in (A), the electron must be residing near the metal surface, primarily in the third region.

systems.[24] The likelihood of the electron encountering a defect can be estimated by comparing the distance an electron travels to the density of defects. The group velocity of an electronic wave is given by eq 3.[25]

$$v_{\mathrm{g}} = \frac{1}{\hbar}\frac{\partial E}{\partial k_{\|}} \tag{3}$$

This corresponds to an initial group velocity of 0−1.5 Å/fs for the crystal momenta experimentally observed (up to 0.2 Å^{-1}), allowing the electron to sample over up to 115 Å. Typical crystalline islands in thiophene oligomers range in size up to hundreds of nanometers, notably longer than the upper bound established by these experiments.[26,27] In addition, there is no point in time in which there exist both delocalized and localized image potential state peaks, as one would expect for electrons being trapped by defects.

Polaron formation, on the other hand, is expected to show a continuous decrease in energy of the peak center as a function of time, as observed here. Previous determinations of small polaron formation were able to verify the mechanism by comparing the relaxation rates of the delocalized electrons at differing parallel momentum.[11]

Recent work by Ku and Trugman suggest that the dynamics of 2D small polaron formation can happen on a time scale as fast as 5 vibrational periods for states with low initial momentum.[28,29] Polaron formation in alkyls has been previously identified as being coupled strongly to the methyl rocking motion at 750 cm^{-1}, which corresponds to a period of 44 fs. Five vibrational periods would be 220 fs, which is the same time scale that we see for localization of the IPS in DH6T. We thus suspect that the state is being localized by self-trapping in alkyl groups, although we cannot definitively rule out trapping by defect sites.

---

(24) Stahler, J.; Meyer, M.; Zhu, X. Y.; Bovensiepen, U.; Wolf, M. *New J. Phys.* **2007**, *9*, 394.

(25) Ashcroft, N. W.; Mermin, N. D. *Solid State Physics*, 1st ed.; Harcourt Inc.: Orlando, FL, 1976.

(26) Ratera, I.; Chen, J.; Murphy, A.; Ogletree, D. F.; Frechet, J. M. J.; Salmeron, M. *Nanotechnology* **2005**, *16*, 235–239.

(27) Hajlaoui, M. E.; Garnier, F.; Hassine, L.; Kouki, F.; Bouchriha, H. *Synth. Met.* **2002**, *129*, 215–220.

(28) Ku, L. C.; Trugman, S. A.; Bonca, J. *Phys. Rev. B* **2002**, *65*, 174306–174316.

(29) Ku, L. C.; Trugman, S. A. *Phys. Rev. B* **2007**, *75*, 104307–104312.

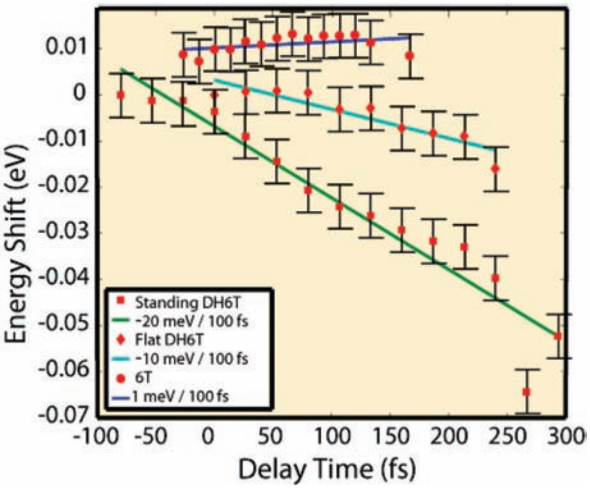

Figure 7. Energetic relaxation of the IPS from its maximal value. Over time, the electron in the IPS reduces its energy by polarizing the medium around it. This is the energy lost to stabilizing the localizing charge. The alkylated molecules show rapid energetic dissipation, but the 6T film remains at constant energy. The 6T data are offset by 0.01 eV for legibility.

Localization of charge carriers reduces the performance of photovoltaics by decreasing maximum voltages as well as reducing currents. Dynamic relaxation of the electron as it distorts and polarizes the surrounding lattice is a mechanism for charge stabilization in the solid state. Heeger and co-workers have shown that the polaron stabilization energy results in a decrease of maximum voltages by 200−300 meV.[30] This reorganizational energy has been shown to be the solid-state equivalent of dipole and charge solvation in liquids.[11,31] The three systems, 6T, flat DH6T, and standing DH6T, have initial IPS binding energies of −0.80, −0.77, and −0.64 eV below the vacuum level, respectively. In 6T, the IPS does not interact dynamically with the molecular lattice, resulting in a constant binding energy of the IPS. The IPS in each of the DH6T systems, however, rapidly decreases in energy in an approximately linear fashion, as shown in Figure 7. For flat DH6T, the $n = 1$ relaxes by 20 meV at a rate of 10 meV/100 fs, and for standing DH6T, the $n = 1$ is stabilized by over 50 meV at a rate of 20 meV/100 fs. It is curious that the flat DH6T shows this dynamic stabilization without localization. One potential explanation is that the IPS electron could be inducing a long-range polarization on the monolayer but the metal/aromatic interaction is so strong that it effectively locks the molecule into place and does not permit the full range of motion necessary to form the small polaron. This, however, is highly speculative and would require further investigation to conclusively determine. Regardless, these rapid dynamic shifts in energy in the DH6T systems imply strong lattice interactions as compared to the 6T system.

The highly ordered morphologies here provide an ideal case for examining limits to mobility. The electron is initially delocalized in all three systems, and there is no evidence of localization in unsubstituted sexithiophene. This eliminates the possibility of localization by intramolecular torsion of the aromatic rings for the IPS, as has been proposed for exciton stabilization in polymeric strands of P3HT.[32] In comparison, for multilayers of DH6T, we see an exponential mass enhancement of the excited electron, which eventually becomes a fully localized state with the same lateral size of two DH6T molecules. Furthermore, the energy of the localized state is stabilized by over 50 meV from the original delocalized state, a measurement difficult to make with purely optical techniques. This energetic stabilization is limited by the short lifetimes and should be much larger for systems with larger charge lifetimes. This energy is lost to heat and is not recoverable for work.

Finally, it is important to mention that the electron localization mechanism observed here in DH6T films could differ significantly from that responsible for small polaron formation in extended polymers. In addition to the increased static disorder in polymeric semiconductors due to structural defects such as chain kinks and chemical impurities present in actual devices, alkylation of polymers occurs in a different position on the carbon rings. In (α,ω)-DH6T, the alkyl subunits are terminal and approximately parallel to the conjugated axis, whereas in polymers the alkyl groups are closer to orthogonal to the polymer backbone. This could lead to a different degree of coupling between the dynamic nuclear motions of the alkyl components and the electronic structure, thus altering the efficiency at which the charges become localized. Further experiments to test the dependence of the localization rate on alkyl position, either by alkylation of the β position or by direct examination of the polymers, are necessary. Here, however, we have provided unambiguous evidence of the ability of the alkyl components in organic semiconductors to localize charges in specific situations.

Conclusion

The electron dynamics presented in this Article represent an important development in understanding the molecular properties behind charge transport in organic semiconductors. We have shown that alkylation of organic semiconductors does play a strong role in electron transport. A nearly free electron remains completely delocalized in unsubstituted sexithiophene, whereas the addition of alkyl ligands results in complete localization. Furthermore, we have measured the rate of energy loss due to this process. The electronic energy stabilizes by over 50 meV within the first 220 fs. As a result of this study, the use of alkyl substitution in polymeric devices should be reexamined. We suggest that molecules that can be processed in solution without alkyl units may make more efficient transistors and photovoltaics. Finally, the techniques and methods utilized in this study of alkyl thiophenes should be widely applicable to studying the dynamics of charge energies and mobilities in other systems.

Acknowledgment. We would like to acknowledge the Material Science division of the Department of Energy for direct funding, and the National Science Foundation for the use of specialized equipment. This work was supported by the Director, Office of Science, Office of Basic Energy Sciences, of the U.S. Department of Energy under Contract No. DE-AC02-05CH11231.

JA1066866

---

(30) Scharber, M.; Mühlbacher, D.; Koppe, M.; Denk, P.; Waldauf, C.; Heeger, A.; Brabec, C. *Adv. Mater.* **2006**, *18*, 789–794.

(31) Liu, S. H.; Miller, A. D.; Gaffney, K. J.; Szymanski, P.; Garrett-Roe, S.; Bezel, I.; Harris, C. B. *J. Phys. Chem. B* **2002**, *106*, 12908–12915.

(32) Wells, N. P.; Blank, D. A. *Phys. Rev. Lett.* **2008**, *100*, 086403−086407.